R. M. Suter
Department of Physics and Materials Science and Engineering,
Carnegie Mellon University,
Pittsburgh, PA 15213
e-mail: suter@andrew.cmu.edu

C. M. Hefferan
e-mail: cheffera@andrew.cmu.edu

S. F. Li
e-mail: sfli@andrew.cmu.edu

D. Hennessy
e-mail: hennessy@anl.gov

C. Xiao
e-mail: changshi.xiao@gmail.com

Department of Physics,
Carnegie Mellon University,
Pittsburgh, PA 15213

U. Lienert
e-mail: lienert@aps.anl.gov

B. Tieman
e-mail: tieman@aps.anl.gov

Advanced Photon Source,
Argonne National Laboratory,
Argonne, IL 60439

Probing Microstructure Dynamics With X-Ray Diffraction Microscopy

We describe our recent work on developing X-ray diffraction microscopy as a tool for studying three dimensional microstructure dynamics. This is a measurement technique that is demanding of experimental hardware and presents a challenging computational problem to reconstruct the sample microstructure. A dedicated apparatus exists at beamline 1-ID of the Advanced Photon Source for performing these measurements. Submicron mechanical precision is combined with focusing optics that yield ≈ 2 *μm high* $\times$ *1.3 mm wide line focused beam at 50 keV. Our forward modeling analysis approach generates diffraction from a simulated two dimensional triangular mesh. Each mesh element is assigned an independent orientation by optimizing the fit to experimental data. The method is computationally demanding but is adaptable to parallel computation. We illustrate the state of development by measuring and reconstructing a planar section of an aluminum polycrystal microstructure. An orientation map of* ~ 90 *grains is obtained along with a map showing the spatial variation in the quality of the fit to the data. Sensitivity to orientation variations within grains is on the order of 0.1 deg. Volumetric studies of the response of microstructures to thermal or mechanical treatment will soon become practical. It should be possible to incorporate explicit treatment of defect distributions and to observe their evolution.* [DOI: 10.1115/1.2840965]

Introduction

Processing and application of polycrystalline materials rely on manipulation and control of defect structures. Defects range from point defects in crystals to grain boundaries to dislocation arrays and even more complex structures in alloy and composite systems. Defects may be static or evolving under the relevant environments. Given the importance of these microstructural quantities, it is startling to realize that there has been essentially no way to probe the evolution of individual defect structures inside of bulk materials. Without the ability to track specific ensembles, both science and technology have relied on statistical characterizations of pre- and postmortem tests on separate samples. While this path has led to considerable understanding, it is clear that gaining the ability to follow structure within three dimensional volumes of material would greatly facilitate a deeper understanding of materials response to perturbations and would yield an enhanced ability to manipulate materials properties.

High energy X-ray diffraction microscopy refers to a collection of synchrotron based measurement techniques [1–4] that can probe internal volumes of macroscopic materials in a nondestructive way and thus can address the issues discussed above. These techniques allow one to nondestructively measure, process, and remeasure volumes of material in order to develop a specific understanding of the rules governing structure evolution. Ideally, one can map microstructure at the level of ensembles of crystalline grains and study the internal structure of individual grains. The nondestructive aspect of the X-ray probe means that structures can be followed as processing steps are applied. Traditional techniques using electron microscopy require serial sectioning; this eliminates the possibility for dynamic studies.

In this paper, we report on the development of experimental facilities at the Advanced Photon Source for measuring the geometry of ensembles of grains and on the application of forward modeling techniques for analyzing such data [2]. We illustrate microscope output by collecting data and generating a map of a single layer of an aluminum polycrystal with roughly 90 well ordered grains. Geometries and internal grain structures are illustrated. Computational issues that will arise with large three dimensional data sets are addressed. While we do not measure dynamic response to processing here, this work paves the way for such measurements since it demonstrates the ability to nondestructively characterize polycrystal microstructure inside of a 1 mm diameter sample.

Experimental Details

The experimental geometry for generating microstructure maps using high energy X-ray diffraction microscopy has been described elsewhere [1,2,5,6]. A line focused beam illuminates a planar section of the sample and diffracted beams are imaged by a high resolution two dimensional detector placed at multiple distances from the rotation axis. Our right-handed coordinate system has the incident beam traveling in the $+x$ direction, the $+z$ axis

Contributed by the Materials Division of ASME for publication in the JOURNAL OF ENGINEERING MATERIALS AND TECHNOLOGY. Manuscript received July 31, 2007; final manuscript received December 19, 2007; published online March 12, 2008. Review conducted by Matthew P. Miller. Paper presented at the Materials Processing Defects 5.

pointing up, normal to the illuminated xy plane of the sample. The sample rotation ω is a right-handed rotation about $+z$. Diffracted beam shapes seen on the detector are projections of cross sections of grains along the propagation direction. By making measurements in which intensity is integrated over a sample orientation interval $\delta\omega$, a continuous range of orientations is covered and many Bragg peaks are observed from each grain. Three dimensional measurements may be made by repeating this procedure after translating the sample along z. The remaining challenge is for software to determine from hundreds of measured diffraction images the nature of the microstructure, including grain orientations, locations, and shapes.

We carry out our measurements at the Advanced Photon Source beamline 1-ID, which is a dedicated high energy beamline. 1-ID has permanent, although developing, hardware available for these measurements. Key components include focusing optics, sample stage, and detector. Focusing is achieved with either a bent silicon Laue crystal [7] or refractive optics coupled with a double bounce bent silicon monochromator [8]. Resultant line focused beams have vertical and horizontal dimensions of $\sim 2\ \mu\text{m} \times 1.3$ mm, respectively. We use an air-bearing precision rotation stage with submicron eccentricity and conning errors. Full 360 deg rotation is possible with small samples and an encoder system yields precise rotation intervals and shutter timing. Translation stages mounted atop the rotation stage permit the centering of samples on the rotation axis. The high spatial resolution imaging detector system is comprised of a scintillator optically coupled to a charge coupled device (CCD) camera. The scintillator is a thin layer of Ce doped YAG crystal whose light is reflected by a 45 deg mirror into a side mounted CCD system. The camera resolution is roughly $4 \times 4\ \mu\text{m}^2$. We plan in the near future to replace the CCD camera with a faster readout and higher resolution system. Currently, the camera readout is the rate limiting factor in data collection; with a new system, we expect the counting time and rotation/translation stage motions to dominate. We also are planning to modify the scintillator and its mount to achieve both better spatial resolution and the ability to pass diffracted beams through the mirror to a downstream, strain sensitive area detector. The latter modification will allow combining microstructure maps with measurements of local strain states.

In the current work, we use 50 keV X-rays focused by the bent silicon Laue crystal. This yields a bandwidth of $\sim 1\%$ and a vertical width of 2.5 μm full width at half maximum [2]. The sample is a 1 mm diameter rod of aluminum 1050 alloy obtained from Alcoa. It was annealed at 500°C for 50 min in order to produce large, well ordered grains. We present here the analysis of data from a single layer of the sample and will soon add five additional layers to make a three dimensional map [9]. Data were collected in two 45 deg "wedges:" We perform 45 contiguous 1 deg integrations (one wedge) then repeat this over another 45 deg interval rotated 90 deg from the first. The same set of integrations is measured at each of three rotation axis-to-detector distances, L =5.11 mm, 7.11 mm, and 9.11 mm. Integration times were 2 s. The purpose of the pair of wedges is to overcome the anisotropy of position resolution caused by the small Bragg angles (and, thus, small projection angles) of high energy X-rays. Each grain is viewed from many perspectives; this yields both signal averaging and isotropic shape resolution for each grain.

Analysis Method

We use a forward modeling analysis method essentially as described in Ref. [2]. This method uses a computer simulation of the sample and the experimental geometry to reconstruct the sample microstructure. The illuminated planar section of the sample is gridded with a triangular lattice and within each triangle, the algorithm searches for crystallographic orientations that generate diffraction that overlaps multiple experimentally observed diffracted beams. Thus, the orientation within each triangular area element is tested against the entire experimental data set. Each

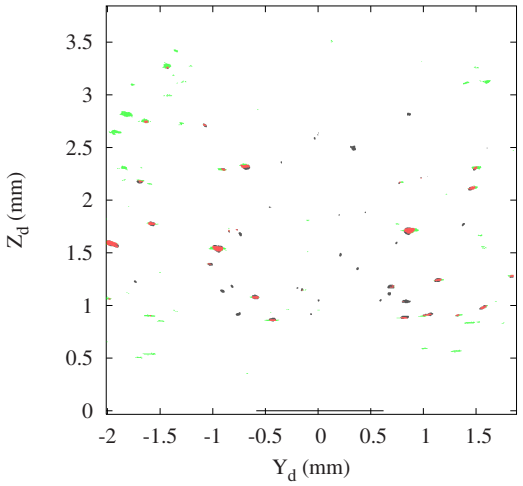

Fig. 1 An example detector image at L=9.11 mm. Black pixels are experimental intensity, green pixels are simulated intensity, and red pixels are both, i.e., red pixels are simulated intensity that overlaps experimental intensity. All diffraction emanates from the intersection of the incident beam with the sample; the direct beam projection onto the detector is shown by the horizontal line at the bottom of the image at z=0. This is one of 270 such images comprising the data set for one layer. See the text for discussion.

simulated Bragg peak is compared to the detector images collected at the ω at which the simulated peak satisfies the Bragg condition. In order for a simulated peak to be said to overlap an experimental diffracted beam, it must strike experimental intensity at each detector distance L for which the simulated beam lies on the detector. A minimum fraction f of such simulated beams must overlap experimental beams in order for the orientation to be accepted. The value of f, which is referred to below as the "confidence" value, is varied from 0.2 to 0.1 during the fitting process, but many elements generate scattering that strikes substantially more than this minimum.

In contrast to the silicon crystal measurements of Ref. [2], here we have grains of different sizes, shapes, and scattering power. We begin the analysis with a coarse triangular grid with a lattice constant comparable to the expected grain size (30 μm) and refine the mesh by halving the lattice constant. In the final iteration, the smallest triangles have 7.5 μm side lengths. Triangles that pass a strong convergence test ($f > 0.75$) and that have neighbors with similar orientations (within 1 deg misorientation) are allowed to converge and are not regridded. The program keeps a list of found orientations and tests new triangles against this list before searching the entire fundamental zone of orientations. If an existing orientation, after Monte Carlo optimization, leads to an acceptable value of f, the blind search process is avoided.

An example detector image corresponding to a fitted data set is shown in Fig. 1. Each of the red regions overlaps experimental intensity not only here but at both L=5.11 mm and 7.11 mm as well. All simulated intensity (both red and green) is generated by clusters of area elements whose orientations have been found to generate numerous other Bragg peaks that track experimental intensity at other ω's. Here, low order scattering near the bottom of the detector is, in the experiment, likely to be absorbed by the beam block. The halo of unmatched simulated scattering toward the top and sides of the image corresponds to high order scattering whose intensity is too small to be observed reliably in this rather low signal level data set. Note that occasional overlap of two Bragg peaks from different grains has little effect on the fitting process. Such overlap usually occurs only at a single distance L and other peaks from each grain appear in nonoverlapped form so

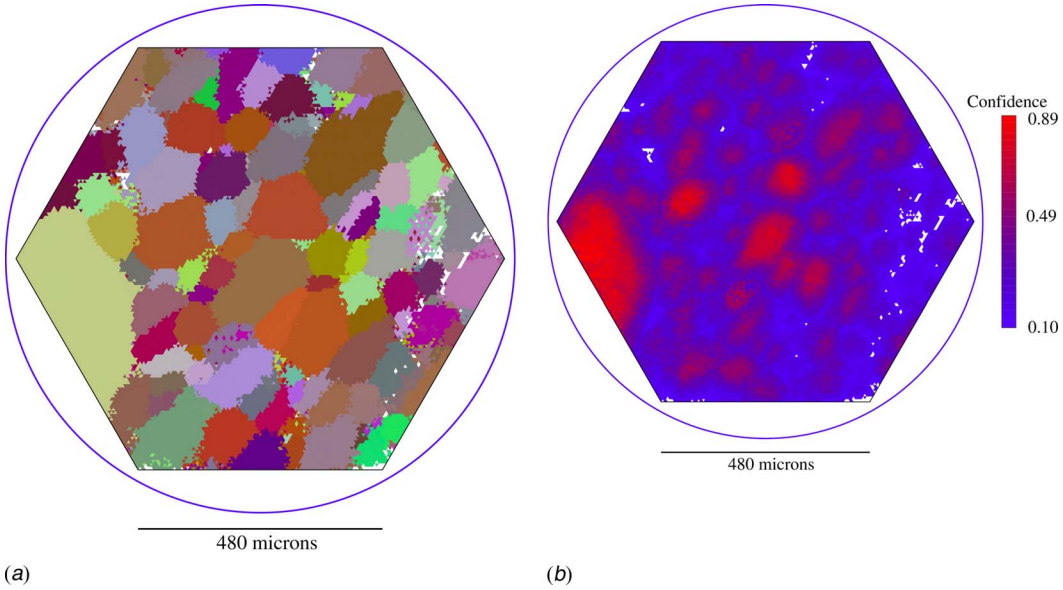

Fig. 2 Reconstructed layer of microstructure of an aluminum 1050 alloy sample. (*a*) shows 24,039 triangular area elements color coded according to their orientations. Regions of apparently uniform color correspond to crystalline grains. White regions were not found to satisfy the convergence criteria for any orientation. (*b*) shows the confidence plot corresponding to the fit in (*a*). The circles show the 1 mm diameter nominal sample size while the hexagons show the simulated sample space. The color orientation scale in (*a*) is arbitrary since the material is isotropic and crystal orientations are measured relative to the arbitrary sample mounting orientation. See the text for discussion.

that shape information is still obtained. The current fits do not use intensity information where overlap may complicate optimization [2].

Results

Figure 2(*a*) shows the reconstructed layer of microstructure. Observed orientations span essentially the entire zone of physically distinguishable values. The number of simulated Bragg peaks that strike at least two detectors varies between 35 and 40 as the crystallographic orientation is varied. This means that red regions in Fig. 2(*b*) have orientations that generate as many as 35 Bragg peaks that match observed diffracted beams. Even with the minimum confidence of $f=0.1$, three or four Bragg peaks match the experiment and this number should be sufficient to specify the local crystallographic orientation. The simulation box (hexagon in Fig. 2) is entirely within the 1 mm diameter sample cross section and this layer is more than a millimeter from the ends of the sample: None of the structure shown could be accessed by traditional methods without cutting the sample open. In the current analysis, we choose to avoid the rather ragged surface of the specimen.

The analysis and graphics algorithms leading to Fig. 2 use no knowledge of grain structure but rather consider area elements as being independent entities. It is reassuring that contiguous regions are found to have similar orientations. Grains are easily picked out by eye as regions of uniform color. In fact, numerous low angle grain boundaries can be identified as subtle color changes across boundaries. Such boundaries have low energy and are expected to be plentiful in a well annealed sample such as this one [10]. From Fig. 2(*b*), we see that confidence levels are high in the centers of grains where diffracted beams strike the centers of observed diffraction spots. Lower confidence occurs near grain edges or grain boundaries where the simulation strikes the edges of observed spots and the details of diffraction line shapes and counting statistics become critical. Essentially, all unfitted white space occurs along grain boundaries and near triple points.

Recognizing that grains should be compact objects, we can easily fill in white spaces to produce a complete structure. The result is shown in Fig. 3. First, we remove any area elements that do not share a side with at least one other element of similar orientation (using 0.75 deg misorientation as the threshold). Next, we allow grains to grow into white space by assigning unfitted element orientations based on a majority rule search of its neighbors. Those with three different neighbor orientations (i.e., those at triple junctions) are given a randomly chosen one of their neighbors' orientations. This process is iterated until all elements have been assigned an orientation. The result is a complete approxima-

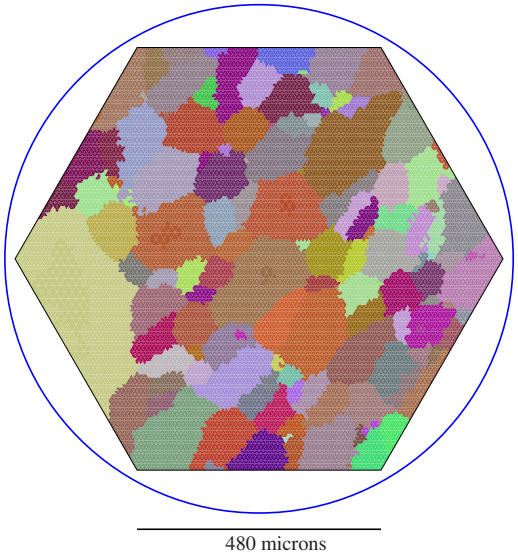

Fig. 3 Optimized microstructure corresponding to the fitted structure of Fig. 2

Table 1 Properties of five grains shown in Fig. 4

Grain	Rotation[a] (deg)	Axis[a]	Area (mm^2)	$\langle \delta\psi \rangle$[b] (deg)	$\delta\psi_{max}$[b] (deg)
1	55.6	(0.74, 0.14, 0.65)	0.052	0.07	0.69
2	39.3	(0.05, 0.16, 0.99)	0.009	0.18	0.52
3	38.7	(−0.24, −0.72, −0.65)	0.024	0.07	0.35
4	43.5	(−0.05, −0.38, −0.92)	0.022	0.07	0.26
5	52.4	(−0.25, −0.68, 0.68)	0.016	0.06	0.57

[a]Angle-axis grain orientations are referenced to cube orientation in the laboratory frame of reference.
[b]Average and maximum misorientation angles.

tion to the microstructure with ≈87 grain cross sections, as shown in Fig. 3. In analysis of adjacent layers [9] (separated in z by 20 μm), we find grains of virtually identical orientation in neighboring locations.

Properties of a few grains are listed in Table 1 and Fig. 4 shows, through expanded color scales, the orientation variations among elements within these grains. Of those listed, only Grain 2 has a significant systematic orientation variation across its cross section. The average misorientation of 0.18 deg is more than twice that of the other grains. As seen in the table, orientation noise appears to be below 0.1 deg on average although much larger fluctuations occur as indicated by the maximum misorientation values. Note that we used $\delta\omega = 1$ deg integration intervals but that the angular resolution of the detector is less than 0.1 deg. Presumably, we could further improve the orientation resolution by using smaller $\delta\omega$.

Computational Challenges

The goal of X-ray diffraction microscopy is to enable studies that follow the dynamics of three dimensional ensembles of grains over the course of various processing steps. While the current results are promising, it must be noted that reconstructing microstructures with the brute force approach used here is computationally challenging and this challenge will grow substantially as larger data sets covering larger volumes of materials and tracking evolution over time become available. Fortunately, our analysis is highly susceptible to massively parallel processing schemes.

As an example of the challenge, consider the measurement at the ultimate resolution goal of 1 μm^3 over a volume of 0.1 mm^3. This represents the specification of orientation in 10^8 volume elements or voxels. If the orientation resolution is even 0.25 deg, there are over 10^7 possible orientations per voxel. The total number of orientation tests becomes 10^{15}! While performing dynamics experiments, it is essential to see how the sample is evolving during data collection so that processing parameters can be tuned accordingly. Thus, rapid analysis during data collection runs is essential.

We use a variety of schemes to reduce the number of tests that have to be made to fit a data set. The triangular grid can be relatively coarse at the beginning of fitting and can then be adaptively regridded based on the stability of convergence on successive iterations and on proximity to rapid orientation changes. Thus, not all area elements need to reach the resolution size. Further, on fitting adjacent layers, the output of one can be used as the starting point for the next. By using a two-tiered convergence criterion, we can insist that any elements that are not high in confidence be refitted—this reduces the influence of the starting orientation assignments as a bias on the fitted structure. Finally, one can imagine (but we have not yet implemented) a scheme in which three dimensional structures are fitted simultaneously. Each layer would be fitted to its own experimental intensity observations but grains could be grown outward in 3D as long as confidence remains high.

In spite of the above shortcuts, computing times will certainly remain long. Hence, we are implementing a parallel computing version of the analysis. Each area element can be fitted entirely independent of others; so, a very large number of processors can work independently. All processors need a copy of the experimental geometrical parameters and the data, which in reduced form is not terribly demanding of memory. Then, given a description of the location and size of one area element, an orientation can be found and passed back to the controlling node. Thus, communication overhead should be quite small and the scaling of clock time with the number of processors should be strong.

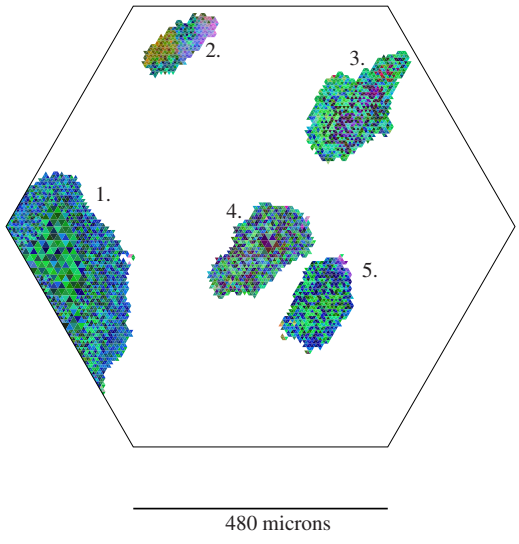

Fig. 4 Five grains shown with expanded color scales so as to allow visualization of intragrain orientation variations. The color scale for each grain is referenced to the average orientation of its elements and shows the misorientation angle and axis of each element from this value. Statistics of these grains are listed in Table 1.

Discussion and Conclusions

We have demonstrated the reconstruction of a single layer of microstructure of a real polycrystal sample from X-ray diffraction microscopy data. Data collected at the Advanced Photon Source beamline 1-ID are reliable enough that we can fit many diffraction peaks observed at widely spaced sample orientations with a single crystallographic orientation. The forward modeling approach and our specific computer code are able to deal with noisy data and a sample with ~90 grains in a cross section. While the computations are slow (the final fit iteration required 50 h on a single 2.8 GHz Xeon processor running LINUX), we are working to implement a parallel version of the code that will take advantage of available massively parallel computer architectures.

General aspects of the reconstruction presented here seem quite robust due to the large number of Bragg peaks that are matched and the fact that independently fitted adjacent layers (not shown here) [9] contain regions with matching orientations. However, the details of grain boundary locations and the completeness of the grain structure need to be tested independently. Since the X-ray measurements are nondestructive, we have the intact sample and are working on serial sectioning measurements using orientation imaging microscopy. This will give us a quantitative calibration of errors in the current maps and, in future work, will allow us to optimize a variety of algorithmic parameters and details.

An analysis of the maximum confidence level achieved within grain cross sections of different areas (see Fig. 2(*b*)) gives some indication of the size resolution of the data set presented here. All grains with areas above 0.01 mm^2 (equivalent circle diameter of 110 μm) have confidence greater than 0.54; this corresponds to

the simulation matching at least 20 experimentally observed Bragg peaks. A smooth curve of confidence versus area passes through 0.3 confidence (a distinct peak above grain boundary regions) at an area of 0.002 mm^2 (equivalent circle diameter of 50 μm). Numerous small clusters of area elements with relative misorientations <0.2 deg have linear dimensions of ≈ 10 μm. Thus, the fit yields some shape information for grains with lengths greater than 50 μm and indicates the presence and location of grains as small as 10 μm. We expect improvements in hardware and in counting statistics to lead to improvements in resolvable lengths by at least a factor of 10.

Because it does not assume any global properties of grains, such as sharp Bragg scattering, our analysis allows us to see internal orientation distributions within grains. While we have illustrated this above, optimal treatments will require consideration of intensity variations over diffraction spots rather than the simple thresholding used here [2]. Since each grain strikes many experimental spots, there exists a large amount of information to constrain reconstructions of internal structures. One way to approach such analysis would start with maps such as presented here, select out data subsets that correspond to a particular grain in three dimensions, and use a Monte Carlo process to move coarse grained parameters describing local lattice distortions. Using subresolution sample gridding generates intensity variations consistent with a particular geometry just by counting the number of voxels that strike specific detector pixels. In the future, this type of analysis can be combined with high angular resolution, strain sensitive measurements to provide an extremely complete description of microstructures.

Acknowledgment

This work was supported primarily by the MRSEC program of the National Science Foundation under Award No. DMR-0520425. Use of the Advanced Photon Source was supported by the U.S. Department of Energy, Office of Science, Office of Basic Energy Sciences, under Contract No. DE-AC02-06CH11357.

References

[1] Poulsen, H. F., 2004, *Three-Dimensional X-Ray Diffraction Microscopy* (Springer Tracts in Modern Physics Vol. 205), G. Hohler, ed., Springer, Berlin.
[2] Suter, R. M., Hennessy, D., Xiao, C., and Lienert, U., 2006, "Forward Modeling Method for Microstructure Reconstruction Using X-Ray Diffraction Microscopy: Single Crystal Verification," Rev. Sci. Instrum., **77**, p. 123905.
[3] Jakobsen, B., Poulsen, H. F., Lienert, U., Almer, J., Shastri, S. D., Sorensen, H. O., Gundlach, C., and Pantleon, W., 2006, "Formation and Subdivision of Deformation Structures During Plastic Deformation," Science, **312**, pp. 889–892.
[4] Margulies, L., Winther, G., and Poulsen, H. F., 2001, "In Situ Measurement of Grain Rotation During Deformation of Polycrystals," Science, **291**, pp. 2392–2394.
[5] Lauridsen, E. M., Schmidt, S., Suter, R. M., and Poulsen, H. F., 2001, "Tracking: A Method for Structural Characterization of Grains in Powders or Polycrystals," J. Appl. Crystallogr., **34**, pp. 744–750.
[6] Poulsen, H. F., Nielsen, S. F., Lauridsen, E. M., Schmidt, S., Suter, R. M., Lienert, U., Margulies, L., Lorentzen, T., and Juul Jensen, D., 2001, "Three-Dimensional Maps of Grain Boundaries and the Stress-State of Individual Grains," J. Appl. Crystallogr., **34**, pp. 751–756.
[7] Lienert, U., Schulze, C., Honkimaki, V., Tschentscher, T., Garbe, S., Hignette, O., Horsewell, A., Lingham, M., Poulsen, H. F., Thomsen, N. B., and Ziegler, E., 1998, "Focusing Optics for High-Energy X-ray Diffraction," J. Synchrotron Radiat., **5**, pp. 226–231.
[8] Shastri, S. D., Almer, J., Ribbing, C., and Cederstrom, B., 2007, "High-Energy X-Ray Optics With Silicon Saw-Tooth Refractive Lenses," J. Synchrotron Radiat., **14**, pp. 204–211.
[9] Hefferan, C. M., Li, S. F., Moore, R., Hennessy, D., Xiao, C., Lienert, U., and Suter, R. M. (unpublished).
[10] Saylor, D. M., El Dasher, B. S., Rollett, A. D., and Rohrer, G. S., 2004, "Distribution of Grain Boundaries in Aluminum as a Function of Five Macroscopic Parameters," Acta Mater., **52**, pp. 3649–3655.